

**Spatial patterns of disconnectivity explain catchment-scale sediment dynamics and transfer efficiencies**

**Authors: Mike Turley<sup>1\*</sup>, Marwan A. Hassan<sup>1</sup>**

<sup>1</sup> Department of Geography, The University of British Columbia, Vancouver, B.C., Canada.

\*Corresponding author: Mike Turley ([mbturley@student.ubc.ca](mailto:mbturley@student.ubc.ca))

**Key Points:**

- Disconnectivity is the dominant but inefficient state of a system in transferring matter and energy within and between system components
- Sources of disconnectivity were found to accurately explain catchment-scale sediment dynamics
- During extreme events, the efficiency of sediment transfer increases resulting in rapid adjustment

## Abstract

While connectivity studies are becoming common in the Earth sciences, disconnectivity has received much less attention. Sediment storage is the direct result of sediment disconnectivity and can provide concrete evidence of the spatial patterns of disconnectivity at the catchment-scale. In this study we explore the catchment-scale sediment dynamics of the Tahoma Creek watershed, a high-gradient glacio-volcanic landscape, within a sediment budget framework and identify and map sources of disconnectivity to determine if they explain the spatial patterns and estimated efficiencies of sediment transfers. We found that up to 80% of the total eroded sediment is sourced from the proglacial zone. The proglacial zone is characterized by high connectivity resulting from frequent debris flows and floods, and rapidly responds to changing conditions. Down valley however, sources of disconnectivity become increasingly more prevalent, the hillslopes become decoupled from the channel, and a majority of the eroded sediment is redeposited with as little as ~15% reaching the outlet. The spatial distribution of sources of disconnectivity and their upslope affected areas explains, to a large degree, catchment-scale sediment dynamics and sediment transfer efficiencies and is in close agreement with quantitative connectivity estimates. We find that steep, glaciated watersheds are predominantly disconnected over human timescales and suggest that disconnectivity is the dominant state of landscapes over most timescales of interest. Mapping sources of disconnectivity provides a straightforward and concrete approach to estimating system disconnectivity and can increase confidence when paired with quantitative indices.

## Plain Language Summary

Mountain watersheds supply freshwater and sediment to downstream river systems, affecting flooding, fish habitat, and water quality. We argue that understanding the spatial and temporal patterns of sediment movement within a landscape requires knowing where and for how long sediment is stored, and the overall efficiency of sediment transfer between different parts of the landscape. We illustrate the importance and utility of mapping landforms and landscape characteristics that delay or disrupt sediment movement using the Tahoma Creek watershed as an example. This watershed drains a portion of Mount Rainier, a volcano shaped by glaciers in Washington, USA, and is incredibly dynamic. We find that landforms and landscape characteristics that limit sediment movement are common, and that mapping them gives an accurate picture of sediment movement patterns. Glaciers dramatically reshape the landscape, which controls sediment supply and movement patterns, and their legacy remains for thousands of years after they retreat. We also make use of high-resolution elevation data representing the land surface in 2002, 2008, and 2012 to quantify how much erosion, transport, and deposition occurred and how efficiently sediment was transported. We find that sediment is transported more efficiently during extreme events, such as the 2006 floods.

## 1 Introduction

Mountain watersheds supply freshwater and sediment to downstream river systems, affecting flooding, fish habitat, and water quality. The movement of water and sediment within a landscape is dependent on coupling between upstream sediment sources and downstream river

systems, and more generally, landscape connectivity. While connectivity is becoming an increasingly popular topic of study (Slaymaker & Embleton-Hamann, 2018; Najafi et al., 2021), investigations that explicitly consider disconnectivity remain relatively uncommon (some key exceptions include: Walling, 1983; Fryirs et al. 2007ab; Fryirs, 2013; Hoffmann, 2015; Grant et al., 2017).

Within the literature, the infrequent and spatially limited nature of mass and energy transfer within systems is often noted (e.g., Hoffmann, 2015; Repasch et al., 2020; Ben-Israel et al., 2022), suggesting that disconnectivity is the more common state of geomorphic systems (an idea explored further in this paper). We define disconnectivity as the dominant but inefficient state of a system in transferring matter and energy within and between system components. This definition modifies previous definitions (Chorley & Kennedy, 1971; Wohl et al., 2018), with additional emphasis on the fragmented and inefficient nature of most landscapes. Disconnectivity occurs as a result of landforms (Fryirs et al., 2007a), bio-geomorphic characteristics of the system (i.e., vegetation [e.g., Cienciala, 2021], slope [e.g., Cavalli et al., 2013], network structure [e.g., Cossart & Fressard, 2017; Gran & Czuba, 2017], etc.), negative process-form feedbacks (Cossart, 2008; Lane et al., 2017), thresholds (Schumm, 1979), and process discontinuity (Grant et al., 2017) that reduce the efficiency of sediment transfer through storage. A consideration of disconnectivity is required to explain sediment storage patterns and landscape morphology (Hoffmann, 2015), interpret sedimentary archives, explain buffering of climatic or tectonic signals and system response times (Tofelde et al., 2021; Ben-Israel et al., 2022), and explain landscape resilience (Fryirs, 2017; Lisenby et al., 2020). Disconnectivity is also required to explain how and why landscapes can be in a state of disequilibrium with current processes and conditions, a fundamental consideration for previously glaciated landscapes (Church & Ryder, 1972; Ballantyne, 2002). Connectivity on the other hand, may be defined as the spatially and temporally limited efficient state of a system in transferring matter and energy within and between system components. Wohl et al. (2018) provides a useful review of the subject, including what we (field of geomorphology) do and don't yet know.

Many mountainous landscapes have been repeatedly reshaped and reorganized by glacial cycles throughout the Quaternary Period. Glacial retreat since the Last Glacial Maximum has resulted in non-glacial processes operating on relict glacial topography and process-form disequilibrium, so that topographic signatures don't match contemporary geomorphic process domains (Brardinoni

& Hassan, 2006). As a result, glacial and postglacial landscapes alike are dynamic, complex, and heterogeneous systems shaped by a variety of processes. Remnant glacial deposits are often thick and unconsolidated, making them important sources of sediment when accessible. In British Columbia, a positive relation was found between specific suspended sediment and drainage area for basins up to 30,000 km<sup>2</sup> due to secondary reworking of glacial sediments (Church & Slaymaker, 1989). Glaciofluvial terraces, for example, have been identified as important sources of sediment in postglacial basins (Reid et al., 2021; Scott & Collins, 2021). While research in postglacial systems has primarily focused on aspects of paraglacial sedimentation (Church & Ryder, 1972), few studies have explored the degree to which glacial landscapes are uniquely and highly fragmented.

It is also important to note that while the term disconnectivity became prevalent only recently, the concept has been inferred for a long time when calculating sediment budgets (Dietrich et al., 1982). A sediment budget is a quantitative description of the rates of production, transport, and export of sediment that incorporates changes in storage, and specifies the contribution from different processes (Dietrich et al., 1982; Reid & Dunne, 1996; Hinderer, 2012; Reid & Dunne, 2016). In conceptualizing the system as a sediment cascade through temporary sediment stores, sediment budgets can reconcile the contemporaneously continuous and discontinuous processes that operate over different timescales (Grant et al., 2017) and therefore facilitate studies of disconnectivity.

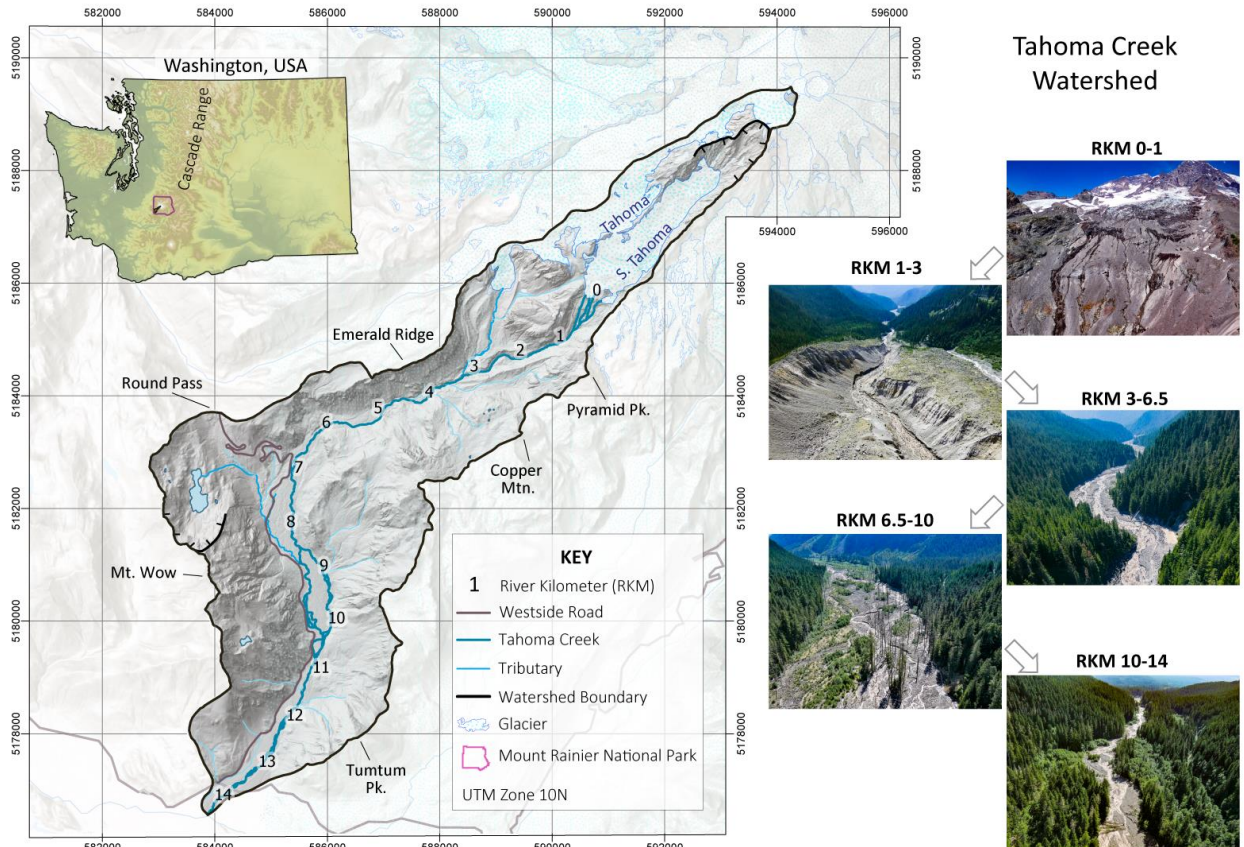
Fryirs et al. (2007a) presents a useful categorization system of sources of disconnectivity. In this system, sources of disconnectivity are classified as buffers, barriers or blankets based on whether they prevent sediment from entering the channel (lateral disconnectivity), disrupt sediment moving along the channel (longitudinal disconnectivity), or prevent vertical reworking of sediment through smothering (vertical disconnectivity), respectively (Fryirs et al., 2007ab; Fryirs, 2013). Disconnectivity is a key property of the system. A given landscape's tectonic and climatic history results in unique valley geometry, spatial organization of landform assemblages, and topographic complexity, which controls the spatial patterns of hillslope-channel coupling and sediment disconnectivity (Hassan et al., 2018). Disconnectivity in turn controls the location and volume of sediment inputs to the channel and subsequently channel morphology, channel geometry, and bed texture (Hassan et al., 2018, Reid et al., 2021). Channel characteristics determine the functioning of the fluvial system including channel stability and migration (Eaton

et al., 2020), flooding and its' geomorphic effectiveness (Al-Ghorani et al., 2022), and aquatic ecosystems (e.g., Cienciala and Hassan, 2013). An understanding of disconnectivity is then required to interpret the system at different scales, both temporal (e.g., geomorphic effectiveness of floods relating to tectonic and glacial cycles), and spatial (e.g., channel bed texture relating to valley geometry). However, the utility of disconnectivity has not been fully explored.

This paper aims to illustrate the link between contemporary processes operating on a mountainous landscape shaped by glaciations, the location, types, and relative abundance of sources of disconnectivity, and the resulting spatial patterns of sediment dynamics and transfer efficiencies. In particular we (i) explore the catchment-scale sediment dynamics of a high-gradient glacio-volcanic landscape within a sediment budget framework utilizing multitemporal high-resolution DEMs and fieldwork data, and (ii) identify and map sources of disconnectivity to determine if they explain the spatial patterns and estimated efficiencies of sediment transfers. We present general descriptions of sources of disconnectivity that might be found in similar high-mountain, glaciated watersheds and discuss the utility of using them to gain understanding of sediment dynamics. The Tahoma Creek watershed is spatially heterogeneous and dynamic, making it an ideal location to illustrate sources of disconnectivity. Additionally, the spatial patterns of sources of disconnectivity are compared to previously published quantitative estimations of connectivity in this basin (Turley et al., 2021).

## 2 Study Site

The Tahoma Creek Watershed drains approximately 40 km<sup>2</sup> of the southwest flank of təq'u?ma? (Mount Rainier), an active stratovolcano within the Cascade Range of Washington, USA, in the territory of the dx<sup>w</sup>sq<sup>w</sup>ali? abš (Nisqually) and spuyaləpabš (Puyallup) tribes (Figure 1). Tahoma Creek emanates from and follows the last glacial maximum (LGM) path carved by the South Tahoma Glacier for ~14 km. Distances are measured along the river's centerline beginning at the 2019 glacier terminus, denoted in "river kilometers – RKM". The river flows through several distinct zones along its' path beginning as multiple meltwater channels flowing over volcanic bedrock ribs and patchy Neoglacial sediments (RKM 0-1) before flowing through a deeply incised, narrow canyon of unconsolidated drift (RKM 1-3). As the river exits the proglacial zone (zone within the Little Ice Age extent; Carrivick & Heckmann, 2017) it is joined by a tributary



**Figure 1: Location map of the Tahoma Creek watershed with selected photos of key valley segments (modified from Turley et al., 2021).**

issuing from a small lobe of the Tahoma Glacier and flows through a moderately confined canyon flanked by forested hillslopes (RKM 3-6.5). This canyon eventually gives way to a broad unconfined valley characterized by mixed terrace, floodplain, and active channel components with dead tree stands recording recent aggradation and channel widening (RKM 6.5-10; Walder & Driedger, 1994ab; Anderson & Pitlick, 2014; Turley et al., 2021). The channel narrows once more and is confined by paired terraces (RKM 10-14) before spilling out on a debris fan that joins the Nisqually River.

## 2.1 A History of Dynamic Change

The contemporary dynamic landscape is primarily the result of episodic andesite lava flows building impressive topographic relief (Fiske et al., 1963) and repeated cycles of glaciers carving valleys, oversteepening valley walls, and leaving behind large volumes of unconsolidated material (Crandell & Miller, 1974). Infrequent, although not rare, large sector collapse events

that mobilize into cohesive lahars are known to occur (Crandell, 1971; Scott et al., 1995). Today, the Tahoma Creek watershed is prone to frequent debris flows that enact rapid geomorphic change, with at least 35 such events since 1967 (Beason et al., 2019; Crandell, 1971; Legg et al., 2014; Richardson, 1968; Walder & Driedger, 1994a, 1994b). In November of 2006, a large atmospheric river dropped around 500 mm of rain on bare slopes over a 3-day period, an amount far higher than any other event since 1920 when records began (Legg et al., 2014; Anderson & Shean, 2021). This event in turn triggered widespread flooding, debris flows and landslides, factoring in heavily to the quantitative sediment budget presented in this study. This dynamic history and spatially heterogeneous nature make the Tahoma Creek watershed an ideal location for this study.

### 3 Methods

#### 3.1 Mapping

Sediment storage landforms, which are physical representations of sediment disconnectivity in the landscape, were mapped in the field at a 1:8,000 scale during the summer of 2019. The upstream affected areas were then estimated based on D8 flow routing using GIS software with the delineated landforms set as targets. Low-gradient areas were defined as having slopes less than or equal to 8 degrees (Nicoll & Brierley, 2016). Both the flow routing and slope estimates were calculated using the 2008 lidar downsampled to 5-meters resolution, which Turley et al. (2021) found to best capture real disconnections. Vegetation was mapped from 1-meter NAIP imagery collected in 2009 through the calculation of the normalized difference vegetation index (NDVI) using a field-verified threshold. Sources of disconnectivity are classified based on the system proposed by Fryirs et al. (2007a), and encompass buffers, barriers, and blankets which affect the lateral, longitudinal, and vertical disconnectivity, respectively.

#### 3.2 Sediment Budgeting

We present both a conceptual and a quantitative sediment budget over human-timescales (~100 years) for the Tahoma Creek watershed based on a compilation of historical records, published literature (Anderson & Pitlick, 2014; Anderson, 2013), and original contributions from this project. For the conceptual budget, sediment sources, sinks, pathways, and transfer processes were noted in the field during the summer of 2019. The sources were then categorized as either primary or secondary in nature. The secondary sources category refers to hillslope or valley

storage components (sinks) that periodically act as sediment sources, while primary sources are the original stores.

The quantitative budget is based on net change analysis using 1-meter lidar from 2002, 2008, and 2012. We restricted our analysis to the valley floor and adjacent active hillslopes, as determined in the field, to avoid unnecessarily including large areas with insignificant change and increased uncertainties. The resulting budget incorporates fluvial and debris flow processes, and bank erosion. The 2008 and 2012 lidar data cover virtually the entire watershed, while the 2002 lidar covers the active channel and adjacent hillslopes from the glacier front to RKM 12.5. For a more complete description of the datasets see Anderson and Pitlick (2014). The lidar datasets were co-referenced using a terrain-matching technique (Anderson & Pitlick, 2014). While acknowledging that as a mass balance approach, sediment budgets should include an accounting of water, sediment, solute, and nutrient fluxes, and that anything less may seriously limit its quality (Slaymaker, 2004) this project is restricted to a description of the coarse fraction of sediment. Here we are primarily concerned with land-forming materials (coarse sediment), which have been the main focus of past literature at Mount Rainier.

### 3.2.1 Sources of Uncertainty

The spatially variable and vertical datum (DEM-based) uncertainties were calculated for each of the sediment budget components following methods outlined in Anderson and Pitlick (2014) and using the Westside Road (Figure 1) as a stable reference location. The spatially variable uncertainty ( $\sigma_{sv}$ ) was estimated by calculating the standard deviation of unresolved errors between the 2002 and 2012 road surfaces. In our case,  $\sigma_{sv}$  was roughly 0.08, which was conservatively increased to 0.3 m, consistent with values from Anderson and Pitlick (2014).

Spatially variable uncertainty was estimated as,  $\sigma_{sv}\sqrt{n}$ , where  $n$  is the area of interest in  $\text{m}^2$ .

The vertical datum uncertainty ( $\sigma_{vd}$ ) was estimated by calculating the mean elevation differences between the 2002 and 2012 road surfaces. In our case,  $\sigma_{vd}$  was approximately 0.017, which we conservatively increased to 0.025 m consistent with Anderson and Pitlick (2014). The vertical datum uncertainty of a given area  $n$  is,  $\sigma_{vd}n$ . Because the area of interest was sufficiently large, the spatially variable component of uncertainty was negligible and was excluded from the estimates.



In addition to DEM-based uncertainty, several other sources of uncertainty exist. Surface lowering associated with the melting of disconnected stagnant ice is likely the single most important source of uncertainty. Areas where aerial imagery or the patterns of surface lowering suggested the presence of buried stagnant ice were excluded from the analysis. Additionally, some sediment sources may have been excluded from the defined limits of the DEM of difference (DoD) analysis. For example, an unknown volume of coarse sediment enters the system at the glacier front but is assumed to be much less than other proglacial sources (Fahnestock, 1963). A large proportion of the sediment directly entering the proglacial channels is likely suspended and dissolved load that is readily exported from the basin causing minimal morphological change. Nevertheless, fine sediment accumulations in backwater areas or floodplains are not uncommon and complicate the assumption that all morphological changes can be attributed to coarse sediment. Minor hillslope sediment sources may have also been excluded from the analysis. However, fieldwork during the summer of 2019 suggested that little sediment entered the channel from the forested hillslopes, a conclusion supported by Anderson and Pitlick (2014). Density differences between eroded sediment and re-stored sediment contributes to additional uncertainty, although is likely less important than those previously mentioned.

## **4 Results**

### **4.1 Qualitative and Conceptual Sediment Budget**

In constructing a sediment budget for the Tahoma Creek watershed, we attempt to assess the relative importance of various processes of sediment transfer and the causes of disconnectivity within the watershed. Significant sources, sinks, and pathways will be discussed in the following paragraphs, while a more complete accounting is conceptualized in Figure 2.

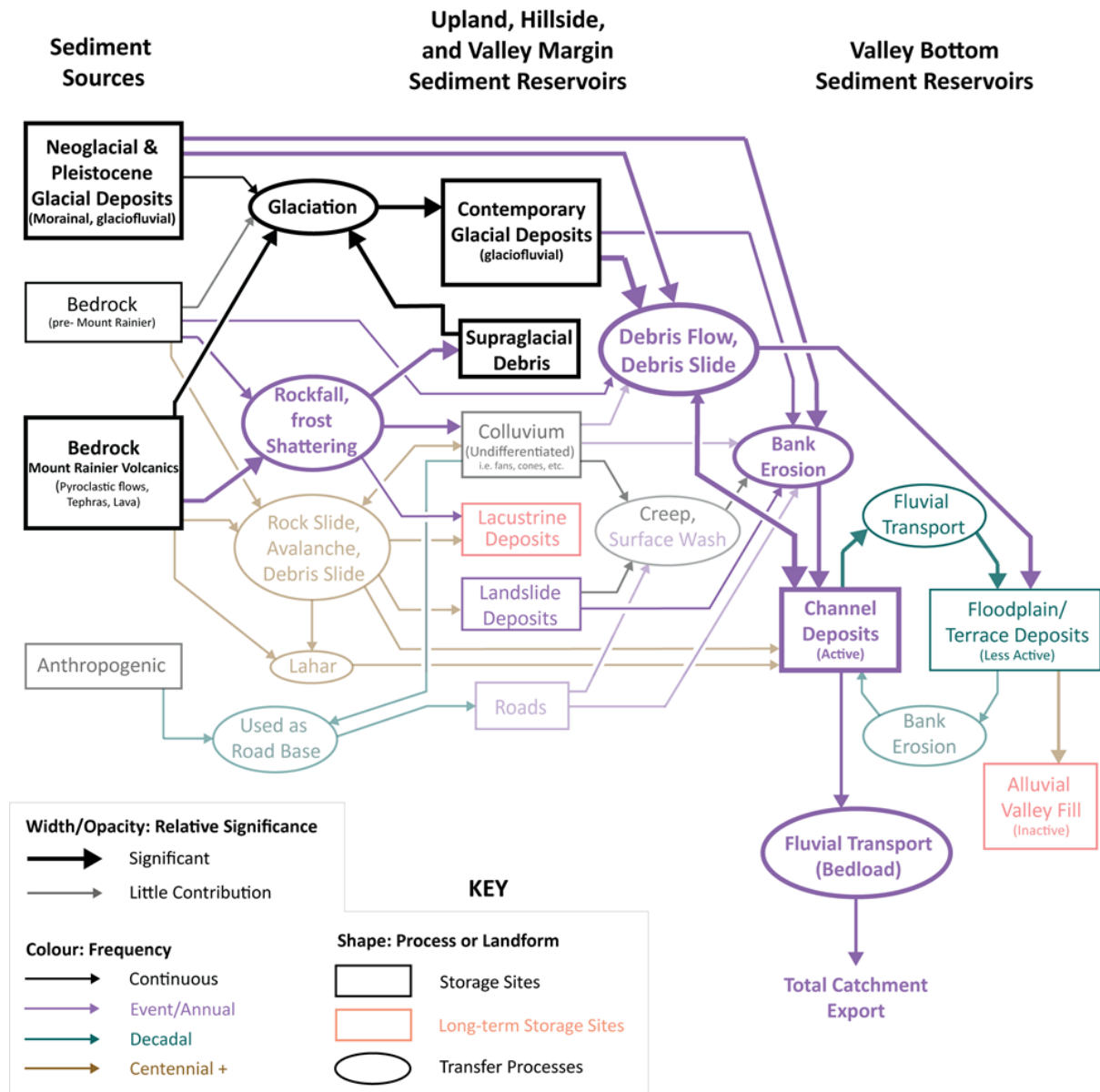


Figure 2: Conceptual coarse sediment budget of the Tahoma Creek watershed.

#### 4.1.1 Sources

##### 4.1.1.1 Primary Sources

The primary sources of sediment within the Tahoma Creek watershed include bedrock (both pre-Mt. Rainier and Mt. Rainier volcanics), glaciogenic sediment, and sediment synthetically added to the system, primarily for road repair (Figure 2). While volcanic eruptions add new volumes of rock and ash, the last known eruption of Mount Rainier occurred 550 to 600 years ago, well outside of the timescale of this study (Fiske et al., 1963). Andesite of the Mount Rainier

volcanics outcrops above the glacier termini in the headwall of the South Tahoma Glacier, along the bedrock ridges dividing the Tahoma, South Tahoma, and Pyramid glaciers, and along many of the ridges forming the watershed divide. This bedrock is the main source of glacial debris. Pre-Mount Rainier bedrock, including the Ohanapecosh and Stevens Ridge Formations as well as intrusive granodiorites and quartz monzonites, dominate the watershed below the glacier termini. Unsurprisingly, basal and ablation till as well as glaciofluvial sediment makes up most of the sediment in the proglacial zone. These primary glacial deposits are easily delineated by the prominent LIA lateral and end moraines. Glaciogenic sediment is the most significant and active source within the watershed at the human-timescale.

#### 4.1.1.2 Secondary Sources

Secondary sources of sediment within the watershed are abundant owing to paraglacial (and proglacial) sedimentation occurring within the valley train and on the adjacent hillslopes. The secondary sources can be further divided into two broad categories in terms of the primary source they are generally derived from and their valley position. The first grouping of secondary sources, those that are primarily derived from bedrock, includes debris avalanche deposits, rock fall deposits, talus, debris cones, and undifferentiated colluvium. These sources generally lie along the lower flanks of the hillslopes and at the hillslope-valley bottom transition. Eight mass movement deposits were mapped within the watershed, five of which are periodically eroded as the river shifts course and undercuts the landforms causing slumping. Undifferentiated colluvium consisting of weathered rock, debris, soil, and vegetation is sourced in the same way. Debris cones lie at the hillslope-valley bottom transition and are sourced through lateral incision at the toe or longitudinal incision by the tributary stream. Talus generally lies higher on the hillslopes directly below rocky cliffs, and seldomly reaches the valley floor. Talus becomes a source of sediment in locations where bedrock outcrops proximal to the valley floor.

The second grouping of secondary sources, derived primarily from glaciogenic sediment within the proglacial zone, includes the active channel, floodplain, terrace, alluvial fan, and debris fan deposits. Debris flow levees would also fit into this category but are relatively less voluminous. Situated on the valley floor, sediment is exchanged between these secondary sources on a regular basis as the river shifts course.

#### 4.1.2 Sinks / Sediment Storage

The secondary sources previously listed alternatively act as sediment sinks. Sediment sinks either partially or completely prevent the transfer of sediment through the system. Different storage landforms operate over varying effective timescales (Fryirs et al. 2007a; Harvey, 2002). For example, within the watershed, lakes are highly effective sediment sinks and operate over millennial timescales. Valley floor aggradation also leads to inactive valley fill deposits that may remain in storage for centuries to millennia. Other sediment storage reservoirs include colluvium (i.e., undifferentiated-debris cones and fans, talus), landslide deposits, alluvial fans, terraces, floodplains, and the active channel.

#### 4.1.3 Pathways – Sediment Production and Transport Processes

Sediment production and transport processes route sediment from source to sink. Figure 2 summarizes the sediment pathways noting the relative significance, and frequency of each process. Frost wedging/shattering occurs throughout much of the year and leads to high rates of rockfall, especially within the South Tahoma Glacier headwall. Glaciers mediate the transfer of rockfall from cirque headwalls to the terminus through slow, continuous transport providing a buffering effect and long-term storage of debris. Erosion primarily occurs within the proglacial zone. During periods of moderate and low magnitude floods, sediment is mainly sourced from the proximal slopes of lateral moraines through periodic gullying at or near the moraine crest and is then temporarily stored along the base in cones or sheets. Shallow translational slides originating near the moraine crest are also likely common (Curry et al., 2009). During larger magnitude floods and debris flows, the sediment accumulations at the base of the moraines are eroded and contribute to bulking of debris flows. Over human-timescales, debris flows and fluvial bank erosion are the two most important processes coupling hillslope sediment sources to the valley floor and eventually the catchment outlet. Many of the other processes only become significant over much longer timescales including, debris avalanches/slides, lahars, and soil creep/tree throw.

#### 4.2 Quantitative Sediment Budget from Multitemporal Lidar

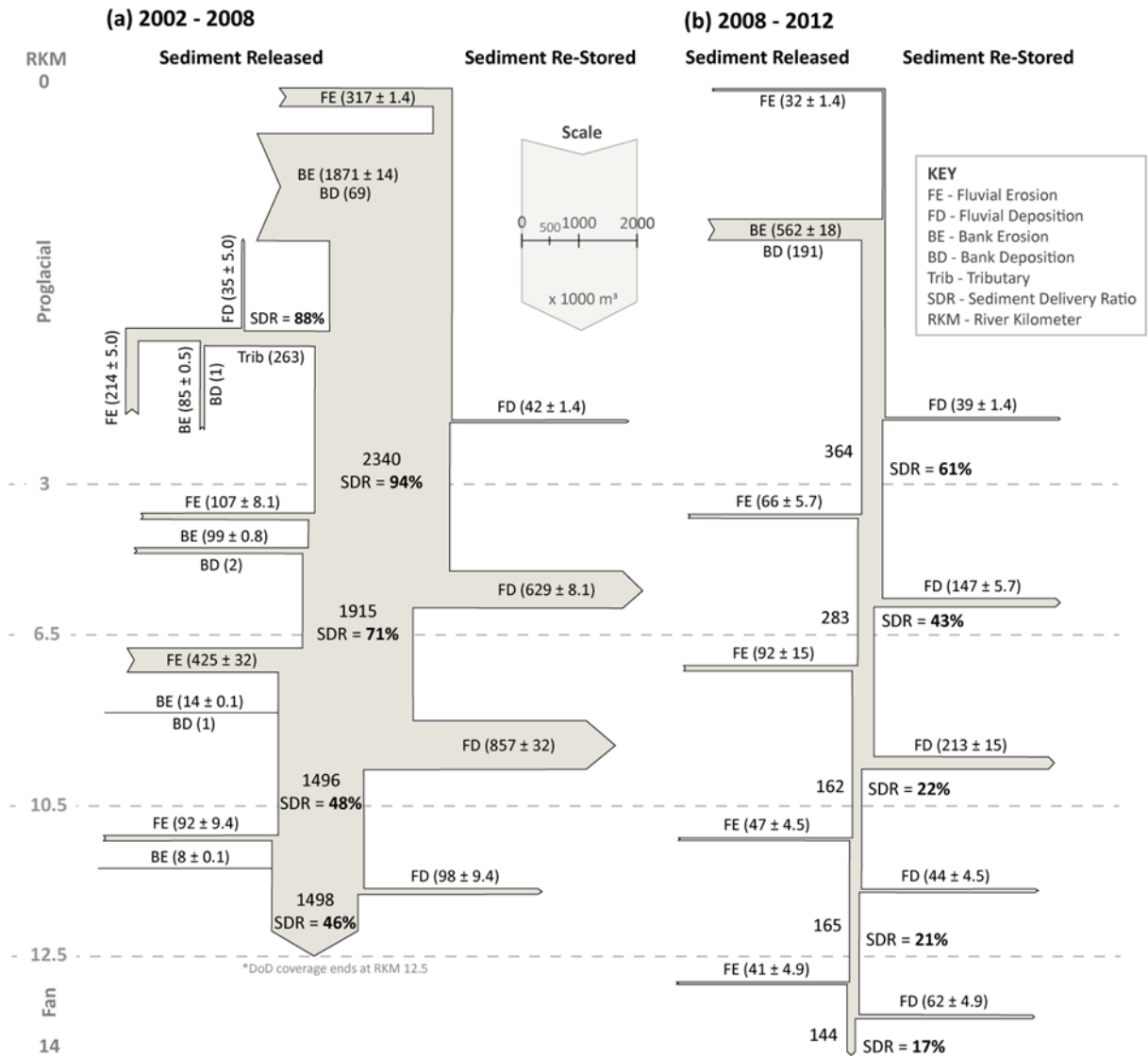
Figure 3 illustrates the estimated coarse sediment budget between 2002-2008 and 2008-2012 based on the DoD analysis (Turley & Hassan, 2023). Between 2002 and 2008 at least  $3232 \pm 71.4 \times 10^3 \text{ m}^3$  of sediment was eroded and  $1734 \pm 71.4 \times 10^3 \text{ m}^3$  of sediment was deposited

within the valley floor. Roughly 80% of the total erosion occurred within the proglacial zone (RKM 0-3), while ~85% of the total deposition occurred between RKM 3-10.5. During this period, an estimated  $1.5 \times 10^6 \text{ m}^3$  ( $250 \times 10^3 \text{ m}^3 \text{ y}^{-1}$ ) of sediment was exported from the watershed.

In contrast, between 2008 and 2012 a minimum of  $840 \pm 49.5 \times 10^3 \text{ m}^3$  of sediment was eroded and  $696 \pm 49.5 \times 10^3 \text{ m}^3$  was deposited within the valley floor. Approximately 70% of the total erosion occurred within the proglacial zone, while 50% of the deposition occurred between RKM 3-10.5. During this period, only  $1.4 \times 10^5 \text{ m}^3$  ( $35 \times 10^3 \text{ m}^3 \text{ y}^{-1}$ ) of sediment was exported from the watershed.

#### 4.2.1 Sediment Delivery Ratios

The sediment delivery ratio (SDR) was calculated every 3-4 kilometers for both periods based on the net export of sediment past a point divided by the gross erosion upstream of that point (Figure 3; Turley & Hassan, 2023). The gross erosion volumes are minimum estimates only and therefore the delivery ratios are maximum estimates. The SDR from the proglacial zone (RKMs 0-3) is 94% for the period 2002-2008, and 61% between 2008 and 2012. The lower delivery ratio in the latter period is a reflection of sediment re-stored at the base of the lateral moraines. The SDR drops to 71% and 43% between RKMs 3-6.5 for the periods 2002-2008 and 2008-2012, respectively. The SDR further drops to 48% and 22% between RKMs 6.5-10 for the 2002-2008 and 2008-2012 periods, respectively. This amounts to approximately a 40% decrease in the SDR between RKMs 3-10.5 for both periods, reflecting the largely depositional nature of this area. Downstream of RKM 10.5 the SDR changes relatively little with erosion approximately balancing out deposition. For the period 2002-2008 the SDR dropped a mere 2% (down to 46%) by RKM 12.5 where the DoD coverage ends. For the 2008-2012 period the SDR is reduced by 1% and then an additional 4% (down to 17%) between RKMs 10.5-12.5 and 12.5-14, respectively. The resulting 25% difference in SDR, as measured at RKM 12.5, between the two periods is largely a result of the temporary storage of eroded sediment at the base of the lateral moraine within the proglacial zone. All other erosion/deposition patterns within each zone remained similar between the two periods.



**Figure 3: Sediment budget for the Tahoma Creek watershed during the (a) 2002 to 2008 period, and the (b) 2008 to 2012 period. Sediment volumes measured from consecutive 1-meter lidar datasets cropped to the active channel and contributing hillslopes. Incorporates fluvial, debris flow processes, and bank erosion processes.**



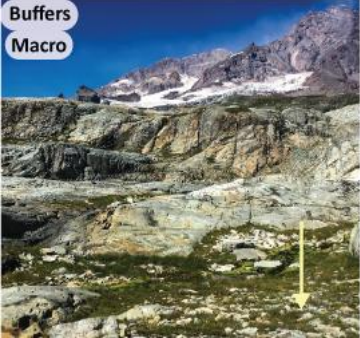
4.3 Sources of Disconnectivity

Disconnectivity is the dominant but inefficient state of a system in transferring matter and energy within and between system components. Sources of sediment disconnectivity are therefore landforms or bio-geomorphic characteristics of the system (i.e., vegetation, slope, network structure, etc.), that reduce the efficiency of sediment transfer through storage. Table 1 provides a general overview of the landforms and bio-geomorphic characteristics that were identified and includes a description of their effects on disconnectivity.


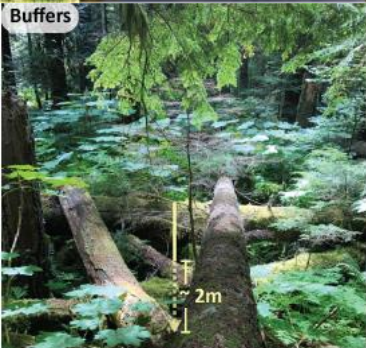

The features identified include lateral moraines, debris flow levees, low gradient areas, lakes, vegetation, terraces/floodplains, fans/cones, roads/culverts/bridges, grain size and competence, in-stream large wood, valley constrictions, and sediment slugs. The location and upstream affected areas of each of the sources of disconnectivity identified within the Tahoma Cr. watershed are visualized in Figure 4 and the respective statistics are summarized in Table 2. Much of the hillslopes and valley bottom terraces are densely forested, while geomorphically active areas lack vegetation. This results in an estimated 57% of the watershed being vegetated including bedrock areas (Table 2). Low gradient areas are primarily located on the valley bottom, but also include hillslope features such as breached divides, cirque floors, and parklands (i.e., low gradient surfaces composed of ancient lava flows scoured by glacial erosion; Riedel & Dorsch, 2016).




Lateral moraines delineate the proglacial zone from RKM 0-3.5 and disconnect ~2% of the watershed. Terraces and floodplains are the two landforms that disconnect the largest proportion of the watershed at 34% and 23% of the total area, respectively (Table 2). They are discontinuous in the upper watershed and become prominent where the valley widens (RKM 6.5), remaining nearly continuous to the outlet. Debris cones and fans, which range in size from a few tens of square meters to nearly a square kilometer, are primarily located between RKMs 7.5 and 12 and together affect approximately 9% of the total basin area (Figure 4; Table 2). Lakes disconnect around 7% of the watershed, with the two biggest being tarns located in glacial cirques in the eastern portion of the basin (Figure 4; Table 2).




363 **Table 1: Description of how specific landforms and bio-geomorphic characteristics increase disconnectivity in (post)glacial**  
364 **watersheds. Includes selected photographs from the Tahoma Creek watershed as examples – taken during the 2019 field**  
365 **season. Photos of fans, valley constrictions, and sediment bulges courtesy of Taylor Kenyon, NPS.**

Landform / Characteristic	Description	Effect on Disconnectivity	Photo
Lateral moraines	Sharp crested linear accumulation of glacially transported rock and debris dropped by the ice along its' lateral margins as it melts.	Cause localized deposition of hillslope sediment on the distal slope of the moraines, while the proximal slope often acts as a sediment supply.	
Debris flow levees	Shear related boundary features resulting from non-cohesive debris flows (Scott et al., 1995). Linear accumulations of sediment that may contain large, downed trees and boulders more than 2 meters across.	Temporarily inhibit the lateral migration of the river, and if located near the valley margin, may prevent hillslope sediment from entering the channel.	
Low gradient	Definitions will vary widely. Defined here as surfaces with < 8° gradient. Hillslope features may include parklands, cirque floors, breached divides, etc. Valley bottom features may include terraces, floodplains, etc. (see other sections).	Results in reduced potential gravitational energy available for sediment transport processes that favor deposition over transport when slope thresholds are not surpassed.	



Landform / Characteristic	Description	Effect on Disconnectivity	Photo
Lakes	Relatively large body of slowly moving or standing water surrounded by land.	Effectively disconnect all upstream areas with respect to coarse sediment, and likely trap a high proportion of the suspended sediment.	
Vegetation	Plants and plant life of an area taken as a whole.	Reduces erosion and promotes deposition and storage by increasing the surface roughness and infiltration, and stabilizing and trapping sediment (Cienciala, 2021).	
Terraces / floodplains	An area of low-lying ground adjacent to a river, formed mainly of river sediments and subject to flooding (Floodplain). Former floodplain surface now elevated above the contemporary channel (Terrace).	Cause localized deposition at the hillslope-valley bottom transition. These landforms are low gradient, and often vegetated (see other sections).	

Landform / Characteristic	Description	Effect on Disconnectivity	Photo
Fans / cones	Fan- or cone-shaped landforms at the hillslope-valley bottom transition composed of sediment deposited by fluvial or mass movement processes.	Buffer hillslope sediment through deposition as the slope decreases. Leenman and Tunncliffe (2020) identified the key up- and downstream controls on fan evolution and buffering capacity as, sediment supply and stream power (upstream), and mainstem aggradation and distal confinement (downstream).	
Roads / culverts / bridges	Anthropogenic infrastructure including flat surfaces prepared for transportation (roads), over a river or other obstacle (bridge), or artificial surface water drainage routing (culverts).	Road's cause localized deposition on the upslope side of roadway due to break in slope. Culverts and bridges limit the lateral mobility of streams and may create backwater areas resulting in deposition upstream of the constriction.	
Grain size / competence	Mass movement and glacial processes are not size selective – sediment delivered to the channel may be too large to be transported.	Coarse deposits limit downstream sediment transport, support persistent aggradation, and may limit vertical reworking as a result of a difference in process competence. The degree of vertical reworking (connectivity) is controlled by the relation between grain size and river competence.	

Landform / Characteristic	Description	Effect on Disconnectivity	Photo
In-stream Large Wood	Logs, sticks, and branches and other wood that protrude or lay within the channel. Generally, > 10 cm in diameter.	Channel spanning log jams create areas of backwater and sediment wedge accumulation. Dead standing trees increase flow resistance and may trap wood and sediment. Large wood often accumulates at the bouldery, and debris-filled snout of debris flows and aids their deposition through increased flow resistance.	
Valley constrictions	Relatively narrow section of the valley bottom. May be the result of glaciation, incision, debris fan progradation, deep-seated landslides entering the valley bottom, etc.	Prevent the river from migrating laterally and can cause backwater areas and aggradation upstream as a result of the bottleneck effect.	
Sediment bulges / slugs	Large fluxes of sediment that can act as plugs within the active channel during low to moderate flows, and thereby limit downstream sediment transport (Nicholas et al., 1995; Fryirs et al., 2007a). May be the result of a single event (e.g., landsliding) or long-term incremental input at a range of spatial scales.	Limit downstream sediment transport and the vertical reworking of sediment by effectively smothering other landforms. Sediment pulse evolution is in part controlled by network structure (Benda et al., 2004), which can enhance or disperse the pulse as a result of synchronization and translation or desynchronization and storage, respectively (Gran & Czuba, 2017).	

**Table 2: Summary statistics of landforms and bio-geomorphic characteristics identified within the Tahoma Cr. watershed and their upstream affected areas.**

Landform/ Characteristic	Coverage Area (km <sup>2</sup> )	Upslope Affected Area (km <sup>2</sup> )	Percent Total Area Affected <sup>1</sup>
Terraces	1.39	9.7	34%
Floodplains	0.86	6.82	23%
Lakes	0.17	1.97	7%
Debris Cones	0.36	1.45	6%
Alluvial Fans	0.04	0.8	3%
Parkland	1.05	-	3%
Moraine Crests	-	0.7	2%
Vegetated <sup>2</sup>	~18.7	-	57%
Slope < 8°	3.64	-	11%
Slope < 4°	1.43	-	4%
Slope < 2°	0.5	-	2%
<b>Total Area Below Glacier Limits (km<sup>2</sup>)</b>	32.9	<sup>1</sup> Based on the actual coverage and upslope affected area of each source of disconnectivity in relation to the total catchment area (below glacier limits). <sup>2</sup> Based on manually verified normalized difference vegetation index (NDVI) value. -Upslope affected area not calculated for parkland or catchment characteristics.	

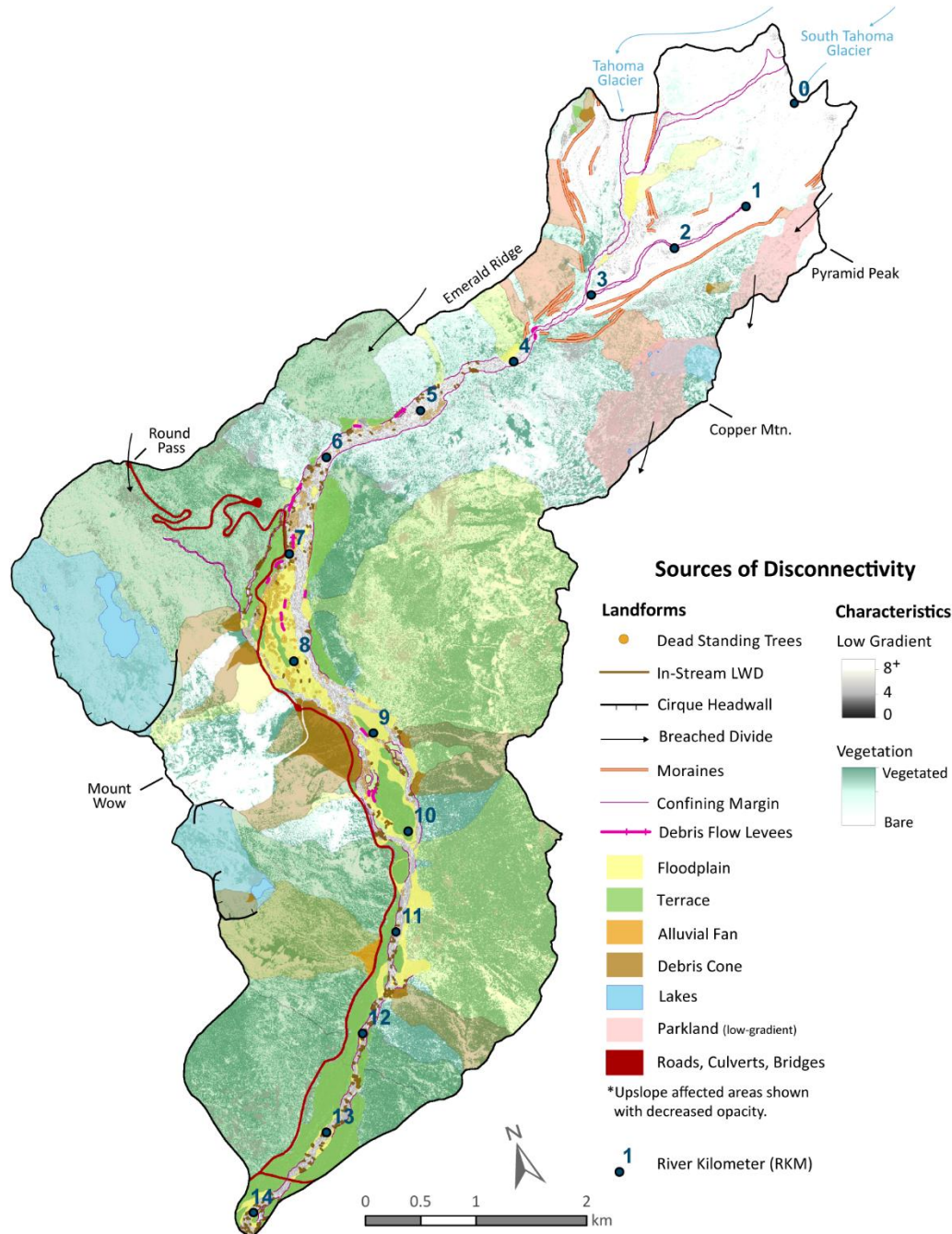
## 5 Discussion

The link between contemporary processes operating on a mountainous glacial landscape, the presence of sources of disconnectivity, and the resulting spatial patterns of sediment dynamics and transfer efficiencies is poorly understood. In this paper, we calculate two quantitative sediment budgets using high-resolution multi-temporal lidar data and identify and map sources of disconnectivity for a 40 km<sup>2</sup> watershed to explore this link. These unique datasets illustrate catchment-scale sediment dynamics and transfer efficiencies, the role of extreme events, and the effective timescales of sources of disconnectivity, each of which are discussed in more detail in this section.

### 5.1 Downstream Trends of Lateral and Longitudinal Disconnectivity

The Tahoma Creek watershed is incredibly dynamic as a result of impressive topographic relief, large stores of unconsolidated glacial sediment in the headwaters, and retreating glaciers that produce glacial outburst floods and debris flows. However, the spatial patterns of sediment sources, pathways, and sinks suggest that the majority of the watershed is in a state of





**Figure 4: Map of sources of disconnectivity and their upstream affected areas. The upstream affected areas are based on D8 flow routing and are displayed in the same color as their associated landform with transparency added.**

385 disconnectivity over human timescales. Active sediment sources are primarily limited to the  
 386 proglacial zone (RKM 0-3), which supplies up to 80% of the total sediment. Sources of  
 387 disconnectivity affect less than 10% of the proglacial area (Figure 5a) which results in the  
 388 efficient transfer of eroded sediment, especially during large events (SDR ~94%). This is in

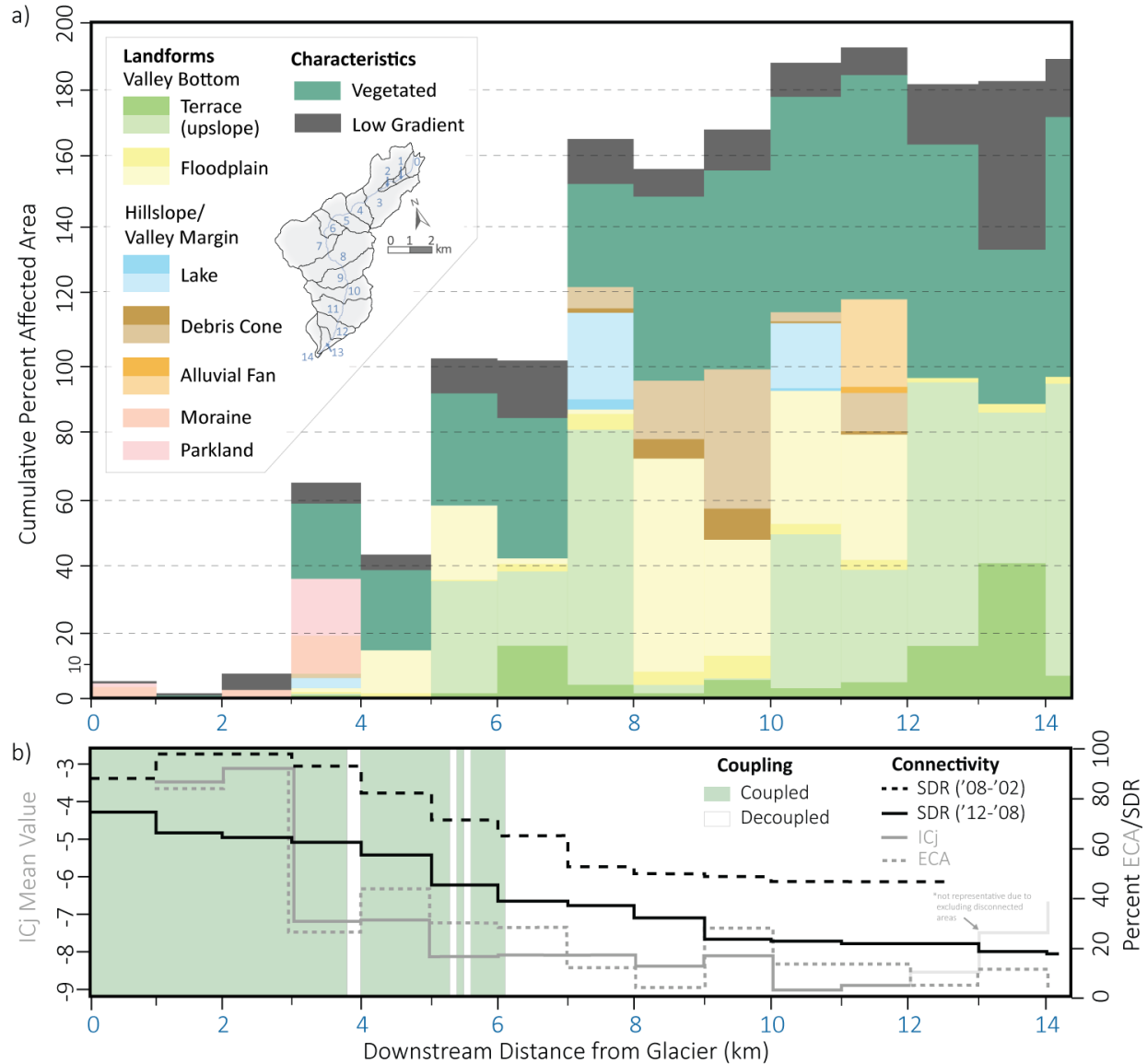
direct agreement with several semi-quantitative indices of connectivity (Figure 5b; Turley et al., 2021).

Down valley, disconnectivity becomes increasingly more prevalent. Between RKM 3-5 the cumulative percent area affected by sources of disconnectivity reaches a moderate 40-60%, the channel becomes net depositional, while the hillslopes remain predominantly coupled to the channel (Figure 5). Between RKM 5-7 in-channel deposition increases reducing the SDR by another 20%, the hillslopes become decoupled from the active channel (~RKM 6; Figure 5b), and the cumulative percent area affected by sources of disconnectivity reaches 100%.

Interestingly, all of the low gradient landforms within the hillslope are a direct result of glaciation (i.e., parklands, breached divides, cirque floors) and significantly increase the cumulative disconnectivity.

Below RKM 7 disconnectivity reaches a maximum with the cumulative percent area affected by sources of disconnectivity reaching 190%, suggesting that most locations are affected by 2 or more sources of disconnectivity (i.e., terraces, vegetation, low gradient). Between RKM 7-10 a substantial amount of in-channel deposition occurs causing the channel to aggrade and reducing the SDR to 22-48%. Over the last half century, this has resulted in several meters of uniform valley aggradation (Walder & Driedger, 1994a; Anderson & Shean, 2021). Below RKM 10, continuous paired terraces completely decouple the hillslopes from the active channel, and connectivity estimates reach a minimum (Figure 5).

The spatial distribution of sources of disconnectivity explains, to a large degree, the estimated structural sediment connectivity (Turley et al., 2021), and catchment-scale sediment dynamics (functional connectivity). The main exception to this finding is the contrasting degrees of functional connectivity between the South Tahoma Glacier meltwater channel (mainstem, RKM 0-3) and the Tahoma Glacier meltwater channel (primary tributary). In this case, debris flows and outburst floods in the mainstem result in significant geomorphic change and functional connectivity, neither of which occur in the tributary valley (Anderson & Shean, 2021). Perhaps unsurprisingly, structural connectivity indices (Turley et al., 2021) were also unable to differentiate between the contrasting degrees of functional connectivity of these two areas. Vegetation, terraces, and floodplains affect the largest portion of the watershed, while lakes are more permanent sediment sinks.



**Figure 5: (a) cumulative percent affected area by sources of disconnection, and (b) longitudinal pattern of connectivity and hillslope channel coupling (modified from Turley et al., 2021). The colors in (a) correspond to figure 4 (this text).**

## 5.2 The Role of Exceptional Events

Several researchers have stated that in proglacial settings the sequencing of extreme events, rather than more frequent lower-magnitude events (e.g., annual rainfall), controls erosion and sediment export over periods of decades and longer (e.g., Anderson & Shean, 2021; Micheletti & Lane, 2016). This conclusion is well supported by evidence from the Tahoma Cr. watershed. The proglacial zone along the mainstem has undergone persistent erosion since 1960, resulting in 50-

80 meters of incision along the ~2 km section of channel (Anderson & Shean, 2021). Walder and Driedger (1994a) document two periods of accelerated erosion. Between 1967 and 1971 at least 8 debris flows scoured the channel by about 5-7 meters. Later, between 1986 and 1992, an additional 15 debris flows/floods occurred and scoured the channel by up to 40 meters. Most of this incision occurred in unconsolidated glacial material. However, Walder and Driedger (1994a) suggest that two debris flows in 1992 scoured a notch into the underlying volcanoclastic bedrock 30-40 meters long and 15-20 meters deep and wide. Debris flows and floods have resulted in the rapid adjustment of the mainstem channel profile to nonglacial conditions.

During the 2002 to 2008 period, an estimated  $1.5 \times 10^6 \text{ m}^3$  ( $250 \times 10^3 \text{ m}^3 \text{ y}^{-1}$ ) of sediment was exported from the watershed, while only  $1.4 \times 10^5 \text{ m}^3$  ( $35 \times 10^3 \text{ m}^3 \text{ y}^{-1}$ ) of sediment was exported between 2008 and 2012. A large debris flow in 2005, and the large 2006 flood and debris flow event are likely responsible for the near order of magnitude difference in sediment transfer volumes. If we assume that an average of  $35 \times 10^3 \text{ m}^3$  of sediment was exported each year during the 2002-2008 period (average for the 2008-2012 period) and that extreme events accomplished the remainder of the sediment export, then as much as 85% of the total sediment exported occurred during these extreme events. This is supported by continuous bed material transport estimates for 1956-2011. Anderson and Pitlick (2014) constructed a synthetic daily hydrograph and two-parameter sediment rating curve for the basin using DoD measurements as volumetric bed material transport values. They estimate that up to 80% of the total bedload transport for the 2002-2012 period, and 50-60% of the total bedload transport for the 1956-2011 period, was accomplished during the 3-day flood in 2006.

Turley et al. (2021) calculated the morphological budget and functional connectivity along the base of the lateral moraines near RKM 2 for both periods (2002-2008, 2008-2012). The volume of exported sediment and functional connectivity estimates were significantly higher for the 2002-2008 period, which they attributed to the high-magnitude flood event in 2006, suggesting event magnitude controls functional connectivity. Our quantitative sediment budget and sediment delivery ratio estimates along the valley bottom support this finding. The delivery ratio was approximately 25% higher and roughly 10 times as much sediment was transported between 2002 and 2008 compared to the 2008-2012 period. During extreme events, thresholds and sources of disconnectivity are surpassed and the efficiency of sediment transfer increases resulting in rapid adjustment.



In contrast, outside of the active channel within the proglacial zone, buffers, barriers, and blankets reduce the efficiency of sediment transfer and sediment storage reservoirs modulate sediment export and signal propagation. In essence, evidence suggests that most of the watershed is in a state of disconnectivity (spatially) most of the time (temporally).

The effect that global warming and glacial retreat will have on sediment dynamics and the importance of sources of disconnectivity isn't entirely clear. However, in documenting debris flow initiation in proglacial gullies during the 2006 flood event at Mt. Rainier, Legg et al. (2014) found slope to be the primary control and suggest that proglacial slopes are often transport limited. Because the glaciers have already retreated onto steep slopes within the Tahoma Creek watershed, debris flow initiation occurs regularly, and large volumes of unconsolidated material, along with easily erodible bedrock provide ample material for downstream bulking. As long as these favorable conditions persist, the frequency of debris flows will likely remain high. As extreme precipitation events become more frequent, and more precipitation falls as rain due to climate change, the frequency of debris flows, and other sediment transport events may increase.

### 5.3 Effective Timescales of Disconnectivity

The effective timescales of disconnectivity features in the Tahoma Creek watershed range between the individual event and tens of thousands of years. Many of the same features noted by Fryirs et al. (2007a) are present in the study area, but additional glacial and debris flow-related features are noted. The effective timescale of glacial sources of disconnectivity also ranges widely. For example, the watershed divides were likely last breached in the late Pleistocene during the Salmon Springs Glaciation (Crandell & Miller, 1974) and have undergone little modification since. In contrast, the lateral moraines were formed much more recently during Neoglacial advances in the 16th and 19<sup>th</sup> centuries (Sigafos & Hendricks, 1972) and are beginning to erode where adjacent to the contemporary channel and will likely operate as buffers on the order of centuries.

Terraces and fans operate as buffers over intermediate timescales. Tree core data from within the watershed suggests that many of the terraces have been stable for several centuries (Anderson, 2013). While recent valley wide deposition (Walder & Driedger, 1994ab) has reactivated many terrace features between RKMs 6 and 10 marked by dead standing trees (Figure 4). Unless valley wide aggradation persists, these terraces will act as buffers for millennia. Researchers have

identified both upstream and downstream controls on fan evolution and buffering effectiveness (Leenman & Tunncliffe, 2020). Key upstream controls are sediment supply and stream power, and key downstream controls are mainstem aggradation and distal confinement. The fans and cones in the Tahoma Creek watershed are fed by ephemeral streams, and therefore downstream (mainstem) controls are likely more important. Valley-wide aggradation and subsequent increased lateral mobility of the mainstem may decrease the buffering effectiveness of these features through erosion of the distal fan margins. Nevertheless, they will remain long-term buffers within the sediment cascade.

In general, within the watershed, blankets operate over shorter timescales than barriers, which in turn operate over shorter timescales than buffers. This is likely the result of buffers often relating to basin-scale macroforms and landforms, both glacial and tectonic in origin, while barriers and blankets are often related more to thresholds, process competence, and smaller more transient biological or anthropogenic structures. As previously noted, the main channel rapidly adjusts both laterally and vertically in response to changing conditions. However, hillslope-channel decoupling and abundant sources of disconnectivity at the valley margins and on the hillslopes delay signal propagation and system response. As a result, hillslope features such as glacial cirques, parkland, and glacial drift deposits persist thousands of years after glacier retreat in a state of disequilibrium with current conditions.

## **6 Implications**

Two primary implications arise from this work. First, the sediment budget presented in Figure 3 illustrates the dependence of sediment budget results on the measurement period. Not only will the total budget volumes reflect the specific set of conditions experienced throughout the measurement period, but the overall patterns of erosion and deposition and subsequently the delivery ratios will also vary. During extreme events, thresholds are surpassed, sources of disconnectivity become less effective at trapping and storing sediment, and the efficiency of sediment transfer increases resulting in rapid adjustment. Sediment budget studies must carefully acknowledge this reality and interpret their results accordingly. More work is needed that links the frequency and magnitude of hydrological and mass movement events to the efficiency of sediment transfer. A better understanding of this link would help define when it is important to consider disconnectivity.

Second, we suggest that mapping sources of sediment disconnectivity can provide a clear picture of sediment dynamics and spatially variable patterns of sediment transfer efficiencies. Among other potential applications, mapping sources of disconnectivity can strengthen and add context when calculating sediment budgets and identifying important sources of sediment or the effective catchment area. Disconnectivity can also help make sense of the spatiotemporal variability of sediment dynamics, especially for transitional systems. Additionally, many sources of disconnectivity can be directly observed and mapped both remotely and in the field, and existing large-scale geomorphic, landform, and terrain classification maps may be reinterpreted in the context of disconnectivity. It is impractical to seek an understanding of catchment-scale sediment dynamics without the explicit consideration of disconnectivity, as it is such a common state of geomorphic systems.

## 7 Conclusions

In this study, we investigate catchment-scale sediment dynamics through sediment budgeting and mapping sources of disconnectivity. The Tahoma Creek watershed drains the southwest flank of Mount Rainier, Washington, USA, and is incredibly dynamic as a result of impressive topographic relief, large stores of unconsolidated glacial sediment in the headwaters, and retreating glaciers that produce glacial outburst floods and debris flows. In constructing a conceptual and quantitative sediment budget, we found that the proglacial zone supplies up to 80% of the total sediment. Frequent debris flows and floods, and high connectivity within the proglacial zone and upper reaches of Tahoma Creek result in a rapid response to changing conditions (i.e., glacier retreat) and intense geomorphic change. However, down valley, the hillslopes become decoupled from the active channel, sources of disconnectivity become increasingly more abundant, and sediment transfer efficiencies decrease resulting in roughly half of the eroded sediment being redeposited. Sediment storage and disconnectivity increase landscape resilience to change and delay, disperse, and disrupt signal propagation. Sources of sediment disconnectivity may persist for thousands of years controlling the spatial patterns of sediment transfers. For example, glacial macroforms such as parklands, glacial cirques, and breached divides persist relatively unchanged in a state of disequilibrium with modern conditions.

We also found that the spatial distribution of sources of disconnectivity and their upslope affected areas explains the spatial patterns of sediment transfers and assumed transfer efficiencies within the watershed. Mapping sources of disconnectivity provides a straightforward approach to estimating system disconnectivity. Even locations with intense morphodynamics, such as Mount Rainier, are predominantly disconnected over human timescales. We therefore suggest that disconnectivity is the dominant state of natural systems and warrants further research. Integrating sources of disconnectivity within connectivity indices or creating an index of disconnectivity would be an interesting avenue of future work. Investigating disconnectivity over longer time periods may also prove useful for understanding landscape evolution, particularly in the context of glacial cycles.

#### **Acknowledgments**

M. Turley was supported by the Department of Geography at the University of British Columbia. Additional funding was provided by a NSERC Discovery Grant (to M. Hassan). Discussions and guidance from Olav Slaymaker motivated and refined this project. This work also benefited from insightful discussions with, and data provided by Scott Anderson. We thank Scott Beason, Taylor Kenyon, and Robby Jost of the U.S. National Park Service at Mount Rainier National Park for assistance with fieldwork preparation and safety planning. We would also like to thank Amy East, and Michéle Koppes for comments on drafts of this work.

#### **Conflict of Interest**

The authors declare that they have no conflicts of interest.

#### **Author Contributions**

The study design was developed by M. Turley and M. Hassan. Data collection and fieldwork was completed by M. Turley. Data analysis was completed by M. Turley under the supervision of M. Hassan. The initial draft and subsequent revisions of the manuscript were completed by M. Turley and M. Hassan.

#### **Data Availability Statement**

Lidar data are openly available through the Washington Department of Natural Resource's lidar portal, available at <https://lidarportal.dnr.wa.gov>. The specific lidar datasets used are entitled, "Rainier West 2002 - DTM", "Rainier 2007 - DTM", and "Rainier 2012 - DTM". The 2009 NAIP imagery is available through the University of Washington, University Libraries WAGDA Image Services, at [https://wagda.lib.washington.edu:6080/arcgis/rest/services/Imagery\\_services/NAIP2009/ImageS](https://wagda.lib.washington.edu:6080/arcgis/rest/services/Imagery_services/NAIP2009/ImageS)

erver. Sediment budget data can be found at Turley and Hassan (2023,  
<https://doi.org/10.6084/m9.figshare.22045217>).

## References

- Al-Ghorani, N. G., Hassan, M. A., & Langendoen, E. J. (2022). Reach-scale morphodynamics: Insights from 20 years of observations and model simulations. *Geomorphology*, 413. <https://doi.org/10.1016/j.geomorph.2022.108375>
- Anderson, S. (2013). Sediment fluxes in a changing climate: Tahoma Creek over daily to centennial time-scales (*Thesis*). University of Colorado at Boulder.
- Anderson, S., & Pitlick, J. (2014). Using repeat lidar to estimate sediment transport in a steep stream. *Journal of Geophysical Research: Earth Surface*, 621–643. <https://doi.org/10.1002/2013JF002933>. Received
- Anderson, S., & Shean, D. (2021). Spatial and temporal controls on proglacial erosion rates: a comparison of four basins on Mount Rainier, 1960 to 2017. *Earth Surface Processes and Landforms*, 1–50. <https://doi.org/10.1002/esp.5274>
- Ballantyne, C. K. (2002). Paraglacial Geomorphology. *Quaternary Science Reviews*, 21, 1935–2017. <https://doi.org/10.1016/B978-0-444-53643-3.00089-3>
- Beason, S. R., Legg, N. T., Kenyon, T. R., Jost, R. P., & Kennard, P. M. (2019). Forecasting and seismic detection of debris flows in pro-glacial rivers at Mount Rainier National Park, Washington, USA. *7Th International Conference on Debris-Flow Hazards Mitigation*.
- Benda, L., Andras, K., Miller, D., & Bigelow, P. (2004). Confluence effects in rivers: Interactions of basin scale, network geometry, and disturbance regimes. *Water Resources Research*, 40, 1–15. <https://doi.org/10.1029/2003WR002583>
- Ben-Israel, M., Armon, M., & Matmon, A. (2022). Sediment Residence Times in Large Rivers Quantified Using a Cosmogenic Nuclides Based Transport Model and Implications for Buffering of Continental Erosion Signals. *Journal of Geophysical Research: Earth Surface*, 127(5). <https://doi.org/10.1029/2021JF006417>
- Brardinoni, F., & Hassan, M. A. (2006). Glacial erosion, evolution of river long profiles, and the organization of process domains in mountain drainage basins of coastal British Columbia. *Journal of Geophysical Research*, 111(F1), F01013. <https://doi.org/10.1029/2005JF000358>
- Cavalli, M., Trevisani, S., Comiti, F., & Marchi, L. (2013). Geomorphometric assessment of spatial sediment connectivity in small Alpine catchments. *Geomorphology*, 188, 31–41. <https://doi.org/10.1016/j.geomorph.2012.05.007>
- Carrivick, J. L., & Heckmann, T. (2017). Short-term geomorphological evolution of proglacial systems. *Geomorphology*, 287, 3–28. <https://doi.org/10.1016/j.geomorph.2017.01.037>
- Chorley, R.J., Kennedy, B.A. (1971). Physical Geography: A Systems Approach. *Prentice-Hall International*, London. 370 pp.
- Church, M., & Slaymaker, O. (1989). Disequilibrium of Holocene sediment yield in glaciated British Columbia. *Nature*, 337(6206), 452–454. <https://doi.org/10.1038/337452a0>

- 620 Church, M., & Ryder, J. M. (1972). Paraglacial Sedimentation: A Consideration of Fluvial  
621 Processes Conditioned by Glaciation. *Geological Society of America Bulletin*, 83, 3059–3072.
- 622 Cienciala, P. (2021). Vegetation and Geomorphic Connectivity in Mountain Fluvial Systems.  
623 *Water*, 13, 593. <https://doi.org/10.3390/w13050593>
- 624 Cienciala, P., & Hassan, M. A. (2013). Linking spatial patterns of bed surface texture, bed  
625 mobility, and channel hydraulics in a mountain stream to potential spawning substrate for small  
626 resident trout. *Geomorphology*, 197, 96–107. <https://doi.org/10.1016/j.geomorph.2013.04.041>
- 627 Cossart, E. (2008). Landform connectivity and waves of negative feed- backs during the  
628 paraglacial period, a case study: The Tabuc sub-catchment since the end of the Little Ice Age  
629 (Massif des Ecrins, France). *Géomorphologie: Relief, Processus, Environnement*, 14(4), 249–  
630 260.
- 631 Cossart, É., & Fressard, M. (2017). Assessment of structural sediment connectivity within  
632 catchments: insights from graph theory. *Earth Surface Dynamics*, 5, 253–268.  
633 <https://doi.org/10.5194/esurf-5-253-2017>
- 634 Crandell, D. R. (1971). Postglacial lahars from Mount Rainier Volcano, Washington. *U. S.*  
635 *Geological Survey Professional Paper*, 667, 80.
- 636 Crandell, D. R., & Miller, R. D. (1974). Quaternary stratigraphy and extent of glaciation in the  
637 Mount Rainier region, Washington. *U. S. Geological Survey Professional Paper*, 59.
- 638 Curry, A. M., Sands, T. B., & Porter, P. R. (2009). Geotechnical controls on a steep lateral  
639 moraine undergoing paraglacial slope adjustment. *Geological Society, London, Special*  
640 *Publications*, 320(1), 181–197. <https://doi.org/10.1144/SP320.12>
- 641 Dietrich, W. E., Dunne, T., Humphrey, N. F., & Reid, L. M. (1982). Construction of Sediment  
642 Budgets for Drainage Basins. In F. J. Swanson, R. J. Janda, Thomas Dunne, & D. N. Swanson  
643 (Eds.), *Sediment budgets and routing in forested drainage basins* (pp. 5–23). Pacific Northwest  
644 Forest and Range Experiment Station, General Technical Report PNW-141.
- 645 Eaton, B. C., MacKenzie, L. G., & Booker, W. H. (2020). Channel stability in steep gravel–  
646 cobble streams is controlled by the coarse tail of the bed material distribution. *Earth Surface*  
647 *Processes and Landforms*, 45(14), 3639–3652. <https://doi.org/10.1002/esp.4994>
- 648 Fahnestock, R. K. (1963). Morphology and hydrology of a glacial stream - White River, Mount  
649 Rainier Washington. *Geological Survey Professional Paper*, 422-A, 1–70.
- 650 Fiske, R. S., Hopson, C. A., & Waters, A. C. (1963). Geology of Mount Rainier National Park,  
651 Washington. *Geological Survey Professional Paper*, 444.
- 652 Fryirs, K. A., Brierley, G. J., Preston, N. J., & Kasai, M. (2007a). Buffers, barriers and blankets:  
653 The (dis)connectivity of catchment-scale sediment cascades. *Catena*, 70(1), 49–67.  
654 <https://doi.org/10.1016/j.catena.2006.07.007>
- 655 Fryirs, K. A., Brierley, G. J., Preston, N. J., & Spencer, J. (2007b). Catchment-scale  
656 (dis)connectivity in sediment flux in the upper Hunter catchment, New South Wales, Australia.  
657 *Geomorphology*, 84(3–4), 297–316. <https://doi.org/10.1016/j.geomorph.2006.01.044>

- 658 Fryirs, K. A. (2013). (Dis)Connectivity in catchment sediment cascades: A fresh look at the  
659 sediment delivery problem. *Earth Surface Processes and Landforms*, 38(1), 30–46.  
660 <https://doi.org/10.1002/esp.3242>
- 661 Fryirs, K. A. (2017). River sensitivity: a lost foundation concept in fluvial geomorphology. *Earth*  
662 *Surface Processes and Landforms*, 42(1), 55–70. <https://doi.org/10.1002/esp.3940>
- 663 Gran, K. B., & Czuba, J. A. (2017). Sediment pulse evolution and the role of network structure.  
664 *Geomorphology*, 277, 17–30. <https://doi.org/10.1016/j.geomorph.2015.12.015>
- 665 Grant, G. E., O'Connor, J., & Safran, E. (2017). Excursions in fluvial (dis)continuity.  
666 *Geomorphology*, 277, 145–153. <https://doi.org/10.1016/j.geomorph.2016.08.033>
- 667 Harvey, A. M. (2002). Effective timescales of coupling within fluvial systems. *Geomorphology*,  
668 44(3–4), 175–201. [https://doi.org/10.1016/S0169-555X\(01\)00174-X](https://doi.org/10.1016/S0169-555X(01)00174-X)
- 669 Hassan, M. A., Bird, S., Reid, D. A., Ferrer-Boix, C., Hogan, D., Brardinoni, F., & Chartrand, S.  
670 M. (2018). Variable hillslope-channel coupling and channel characteristics of forested mountain  
671 streams in glaciated landscapes. *Earth Surface Processes and Landforms*, 16.  
672 <https://doi.org/10.1002/esp.4527>
- 673 Hinderer, M. (2012). From gullies to mountain belts: A review of sediment budgets at various  
674 scales. *Sedimentary Geology*, 280, 21–59. <https://doi.org/10.1016/j.sedgeo.2012.03.009>
- 675 Hoffmann, T. (2015). Sediment residence time and connectivity in non-equilibrium and transient  
676 geomorphic systems. *Earth-Science Reviews*, 150, 609–627.  
677 <https://doi.org/10.1016/j.earscirev.2015.07.008>
- 678 Lane, S. N., Bakker, M., Gabbud, C., Micheletti, N., & Saugy, J.-N. (2017). Sediment export,  
679 transient landscape response and catchment-scale connectivity following rapid climate warming  
680 and Alpine glacier recession. *Geomorphology*, 277, 210–227.  
681 <https://doi.org/10.1016/j.geomorph.2016.02.015>
- 682 Leenman, A., & Tunncliffe, J. F. (2020). Tributary-junction fans as buffers in the sediment  
683 cascade: a multi-decadal study. *Earth Surface Processes and Landforms*, 45(2), 265–279.  
684 <https://doi.org/10.1002/esp.4717>
- 685 Legg, N. T., Meigs, A. J., Grant, G. E., & Kennard, P. (2014). Debris flow initiation in proglacial  
686 gullies on Mount Rainier, Washington. *Geomorphology*, 226, 249–260.  
687 <https://doi.org/10.1016/j.geomorph.2014.08.003>
- 688 Lisenby, P. E., Fryirs, K. A., & Thompson, C. J. (2020). River sensitivity and sediment  
689 connectivity as tools for assessing future geomorphic channel behavior. *International Journal of*  
690 *River Basin Management*, 18(3), 279–293. <https://doi.org/10.1080/15715124.2019.1672705>
- 691 Micheletti, N., & Lane, S. N. (2016). Water yield and sediment export in small, partially  
692 glaciated Alpine watersheds in a warming climate. *Water Resources Research*, 52(51), 5974–  
693 5997. <https://doi.org/10.1002/2016WR018977>
- 694 Najafi, S., Dragovich, D., Heckmann, T., & Sadeghi, S. H. (2021). Sediment connectivity  
695 concepts and approaches. *Catena*, 196, 104880. <https://doi.org/10.1016/j.catena.2020.104880>

- 696 Nicholas, A. P., Ashworth, P. J., Kirkby, M. J., Macklin, M. G., & Murray, T. (1995). Sediment  
697 slugs: Large-scale fluctuations in fluvial sediment transport rates and storage volumes. *Progress*  
698 *in Physical Geography*, 19(4), 500–519. <https://doi.org/10.1177/030913339501900404>
- 699 Nicoll, T., & Brierley, G. J. (2016). Within-catchment variability in landscape connectivity  
700 measures in the Garang catchment, upper Yellow River. *Geomorphology*, 277, 197–209.  
701 <https://doi.org/10.1016/j.geomorph.2016.03.014>
- 702 Reid, Leslie & Dunne, Thomas. (1996). Rapid Evaluation of Sediment Budgets.
- 703 Reid, L.M. and Dunne, T. (2016). Sediment budgets as an organizing framework in fluvial  
704 geomorphology. In *Tools in Fluvial Geomorphology* (eds G.M. Kondolf and H. Piégay).  
705 <https://doi.org/10.1002/9781118648551.ch16>
- 706 Reid, D. A., Hassan, M. A., & McCleary, R. J. (2021). Glacial landscape configuration  
707 influences channel response to flooding. *Earth Surface Processes and Landforms*.  
708 <https://doi.org/10.1002/esp.5240>
- 709 Repasch, M., Wittmann, H., Scheingross, J. S., Sachse, D., Szupiany, R., Orfeo, O., Fuchs, M.,  
710 & Hovius, N. (2020). Sediment Transit Time and Floodplain Storage Dynamics in Alluvial  
711 Rivers Revealed by Meteoric 10Be. *Journal of Geophysical Research: Earth Surface*, 125(7), 1–  
712 19. <https://doi.org/10.1029/2019JF005419>
- 713 Richardson, D. (1968). Glacier Outburst Floods in the Pacific Northwest. *U. S. Geological*  
714 *Survey Professional Paper*, 600-D, D79–D86.
- 715 Riedel, J., & Dorsch, S. (2016). Geomorphology of Mount Rainier Landform Mapping at Mount  
716 Rainier National Park, Washington. *Natural Resource Report*, 1234.
- 717 Schumm, S. A. (1979). Geomorphic thresholds: the concept and its applications. *Transactions of*  
718 *the Institute of British Geographers*, 485–515.
- 719 Scott, D. N., & Collins, B. D. (2021). Frequent Mass Movements from Glacial and Lahar  
720 Terraces, Controlled by Both Hillslope Characteristics and Fluvial Erosion, are an Important  
721 Sediment Source to Puget Sound Rivers. *Water Resources Research*.  
722 <https://doi.org/10.1029/2020wr028389>
- 723 Scott, K. M., Vallance, J. W., & Pringle, P. T. (1995). Sedimentology, Behavior, and Hazards of  
724 Debris Flows at Mount Rainier, Washington. *Geological Survey Professional Paper*, 1547.
- 725 Sigafoos, R. S., & Hendricks, E. L. (1972). Recent Activity of Glaciers of Mount Rainier,  
726 Washington. *Geological Survey Professional Paper*, 387-B.
- 727 Slaymaker, O. (2004). Mass balances of sediments, solutes and nutrients: The need for greater  
728 integration. *Journal of Coastal Research*, SPEC. ISS. 43, 109–123.
- 729 Slaymaker, O., & Embleton-Hamann, C. (2018). Advances in global mountain geomorphology.  
730 *Geomorphology*, 308, 230–264. <https://doi.org/10.1016/j.geomorph.2018.02.016>
- 731 Tofelde, S., Bernhardt, A., Guerit, L., & Romans, B. W. (2021). Times associated with source-  
732 to-sink propagation of environmental signals during landscape transience. *Frontiers in Earth*  
733 *Science*, 9, 1–26. <https://doi.org/10.3389/feart.2021.62831>
- 734 Turley, M., & Hassan, M. A. (2023). Datasets for quantitative sediment budget analysis: Tahoma  
735 Creek Watershed, WA, USA. [dataset]. <https://doi.org/10.6084/m9.figshare.22045217>



- 736 Turley, M., Hassan, M. A., & Slaymaker, O. (2021). Quantifying sediment connectivity: Moving  
737 toward a holistic assessment through a mixed methods approach. *Earth Surface Processes and*  
738 *Landforms*, 46(12), 2501–2519. <https://doi.org/10.1002/esp.5191>
- 739 Walder, J. S., & Driedger, C. L. (1994a). Rapid Geomorphic Change Caused by Glacial Outburst  
740 Floods and Debris Flows along Tahoma Creek, Mount Rainier, Washington, U.S.A. *Arctic and*  
741 *Alpine Research*, 26(4), 319–327.
- 742 Walder, J. S., & Driedger, C. L. (1994b). Geomorphic Change Caused by Outburst Floods and  
743 Debris Flows at Mount Rainier, Washington, with Emphasis on Tahoma Creek Valley. *Water-*  
744 *Resources Investigations Report*, 93–4093.
- 745 Walling, D. E. (1983). The Sediment Delivery Problem. *Journal of Hydrology*, 65, 209–237.
- 746 Wohl, E. E., Brierley, G. J., Cadol, D., Coulthard, T. J., Covino, T., Fryirs, K. A., Grant, G. E.,  
747 Hilton, R. G., Lane, S. N., Magilligan, F. J., Meitzen, K. M., Passalacqua, P., Poepl, R. E.,  
748 Rathburn, S. L., & Sklar, L. S. (2018). Connectivity as an emergent property of geomorphic  
749 systems. *Earth Surface Processes and Landforms*. <https://doi.org/10.1002/esp.4434>